Cellular distribution of the histamine H_3 receptor in the basal ganglia: Functional modulation of dopamine and glutamate neurotransmission

Marta González-Sepúlveda, Santi Rosell*, Hanne M. Hoffmann[1,*], Mª del Mar Castillo-Ruiz, Virginie Mignon [2], David Moreno-Delgado, Michel Vignes [1], Jorge Díaz [2], Josefa Sabriá and Jordi Ortiz

Neuroscience Institute and Department of Biochemistry and Molecular Biology, School of Medicine, Universitat Autonoma de Barcelona, Bellaterra, Spain.

[1] Oxidative Stress and Neuroprotection, IBMM, CNRS UMR-5247, University of Montpellier II, Place E. Bataillon, 34095 Montpellier Cedex 5, France.

[2] Université Paris Descartes and INSERM U-894, Neurobiologie et Pharmacologie Moléculaire, Paris, France

* Both authors contributed equally to this paper

Correspondence:

Jordi Ortiz

Neuroscience Institute and Department of Biochemistry and Molecular Biology

School of Medicine, Room M2-113

Universitat Autonoma de Barcelona,

08193 Bellaterra

Spain

E-mail: jordi.ortiz@uab.es

Telephone: +34935814827

Fax: +34935811573

This version is the Accepted Author Manuscript of Basal Ganglia 3 (2013) 109–121

For the published version of this paper go to http://dx.doi.org/10.1016/j.baga.2012.12.001

Abstract:

Histamine H_3 receptors (H_3R) are widely expressed in the brain where they participate in sleep-wake cycle and cognition among other functions. Despite their high expression in some regions of the basal ganglia, their functional role in this forebrain neural network remains unclear. The present findings provide *in situ* hybridization and immunohistochemical evidence for H_3R expression in several neuronal populations of the rat basal ganglia but not in astrocytes (glial fibrillary acidic protein immunoreactive cells). We demonstrate the presence of H_3R mRNA and protein in dopaminergic neurons (tyrosine hydroxylase positive) of the ventral tegmental area and substantia nigra. In the dorsal and ventral (nucleus accumbens) striatal complex we show H_3R immunoreactivity in cholinergic (choline acetyltransferase immunoreactive) and GABAergic neurons (substance P, proenkephalin or dopamine D_1 receptor positive) as well as in corticostriatal terminals (VGLUT1-immunoreactive). Double-labelling experiments in the medial prefrontal cortex show that H_3R is expressed in D_1R-positive interneurons and VGLUT1-positive corticostriatal output neurons. Our functional experiments confirm that H_3R ligands modulate dopamine synthesis and the probability of glutamate release in the striatum from cortico-striatal afferents. The presence of H_3R in such different neuronal populations and its involvement in the control of striatal dopaminergic and glutamatergic transmission ascribes a complex role to H_3R in the function of the basal ganglia neural network.

Abbreviations

Acb: nucleus Accumbens; D1R: dopamine receptor 1; H3R: histamine receptor 3; PE: proenkephalin; SNc: substance nigra pars compacta; SNr: substance nigra pars reticulata; SP: substance P; SSC: sodium saline citrate; TBS: 50mM tris buffer saline pH 7.6; TSA: tyramide signal amplification; VGLUT1: vesicular glutamate transporter 1 ; VTA: ventral tegmental area

Keywords
histamine H_3 receptor; colocalization; dopamine; electrophysiology;

Introduction

Histamine is involved in a variety of brain functions such as the sleep-wake cycle, attention, learning, memory and the control of food intake and locomotion [1,2] through its interaction with four identified G-protein coupled receptors. Three of them (H_1 to H_3) are widely distributed in the central nervous system while the H_4 receptor is expressed mostly in bone marrow and leukocytes, displaying very low levels in brain [3,4].

The histamine H_3 receptor (H_3R) was initially described as an autoreceptor controlling histamine release and synthesis in histaminergic terminals of the central

nervous system [5,6]. Later, its heteroreceptor role was demonstrated as it also modulates the release of other neurotransmitters including serotonin [7], norepinephrine [8], dopamine [9], glutamate [10] and GABA [11] in brain samples. Many human and rat H_3R mRNA isoforms are generated by differential splicing [12]. In the rat, four isoforms are functionally active: $H_{3(445)}$, $H_{3(413)}$, $H_{3(410)}$, $H_{3(397)}$. $H_{3(413)}$ has been suggested to be the autoreceptor of histaminergic neurons [13]. The H_3R isoforms have a heterogenous expression level in cerebral structures [14] being highly expressed in cortex, thalamus and caudate-putamen [15]. This regional localisation matches the relative distribution of histaminergic projections arising from the tuberomammillary nucleus. In addition, radioligand binding studies in rodents show high H_3R levels in olfactory nucleus, cortex, substantia nigra pars reticulata (SNr), amygdala, thalamus and hypothalamus, specially in tuberomammillary nucleus, with the highest density in striatum and nucleus accumbens [16].

The rat striatum is the main input structure of the basal ganglia involved in sensory-motor behavioural coordination. It can be divided in dorsal and ventral regions: Dorsal striatum (caudate-putamen) has been implicated in the initiation and development of a voluntary motor behaviour, while the ventral striatum (nucleus accumbens, Acb) plays a central role in motivated and goal directed behaviours because it integrates information from motor and limbic systems [17]. Dorsal and ventral striatum differ in afferences and efferences, but both present the same neuronal phenotypes. Thus 95% of striatal neurons are GABAergic spiny projection neurons, which can be divided in two populations: striato-nigral pathway neurons which show dynorphin, substance P (SP) and D_1-like dopamine receptors and striato-pallidal pathway neurons that coexpress enkephalin and the D_2-like dopamine receptor [18,19]. Nevertheless, discrimination between these two populations is not absolutely clear because all of these neurons can express low levels of characteristic receptors of the other neuronal type [20, see also 21]. The remaining 5% of striatal neurons is composed by interneurons of two subtypes: cholinergic and GABAergic [22].

Striatal neurons are a major target of mesencephalic dopaminergic neurons, which are implicated in complex neurological and psychiatric disorders such as Parkinson, Huntington, schizophrenia and addiction. The role of H_3R in normal striatal functions such as locomotion control is not clearly elucidated [23,24], and even less in pathological conditions. However, the therapeutic potential of H_3R antagonists is being studied in sleep-wake disorders, dementia, attention-deficit hyperactivity disorders, and schizophrenia [25,26]. Conversely, stimulation of H_3R decreases L-dopa-induced chorea and turning behaviour in animal models of Parkinson's disease [27,28]. In the present work functional histamine H_3R expression in basal ganglia neuronal populations is studied to evaluate the possibility that H_3 receptors constitute new targets for treatments of these disorders.

Experimental procedures

Tissue preparation for histochemistry

Experiments performed in the present study conformed to the Ethics Committee for Human and Animal Research (Universidad Autónoma de Barcelona) in accordance with the European Communities Council Directive of 24 November 1986 (86/609/EEC). Brains were obtained from male OFA-Sprague-Dawley

rats weighing 200-250 g (Animal Service, Universidad Autónoma de Barcelona, Barcelona, Spain). Animals were sacrificed by decapitation, their brain was removed rapidly, immediately frozen (-40ºC) by immersion in isopenthane and stored at -20ºC. Brain sections (10µm) were prepared on a cryostat and thaw-mounted onto Superfrost slides. Slices were fixed for 40 min at 4ºC in freshly prepared 4% formaldehyde made up in 0.1M phosphate buffer pH 7.4, rinsed three times (5 min each) in 0.1M phosphate buffered saline, pH 7.4, dehydrated through graded ethanol and dried. All the sections were stored at -20ºC until use.

Fluorescent *in situ* hybridization histochemistry

Brain sections were incubated at 37ºC for 10 min with proteinase K (5µg/ml), acetylated for 10 min (in 0.1M triethanolamine, pH 8 and 0.25% acetic anhydride) at room temperature and dehydrated in graded ethanol up to 100%. Hybridization was performed overnight at 55ºC in the presence of 10-20 ng of biotin/digoxigenine labelled antisense or sense probes in hybridization buffer (50% formamide, 10% dextran sulfate, standard saline citrate 2x (SSC), 1% Denhart's solution, 50mM Tris-HCl buffer, 0.1% NaPPi, 0.2mg/ml tRNA, 1mM EDTA). Subsequently, sections were rinsed with: 50% formamide in SSC2x (30 min at 55ºC), SSC2x (5 min at 55ºC, 2 times 10 min at room temperature) and incubated for 40 min at 37ºC with ribonuclease. Then, sections were washed in graded SSC (4x and 2x, 15min each, 0.1x 30 min at 60ºC and 0.1x 10 min room temperature), Tris buffered saline 50mM pH 7.6 (TBS) –Tween 20 0.05% three times (5 min each) and blocked with 1% blocking reagent (Roche Applied Science) in TBS for 1 h at 37ºC. They were then incubated for 2 h at room temperature in a humid chamber with the primary antibodies sheep anti-digoxigenine–peroxidase (Roche Applied Science, 1/100) and mouse anti-Biotin (Jackson Immunoresearch, 1/200) diluted in buffer (TBS, 0.1% acetylated bovine serum albumin, 1% goat serum, 0.1% Tween 20). After three rinses with TBS-Tween 20 0.05% (5 min each) sections were incubated with the green secondary antibody anti-mouse-Alexa488 (Invitrogen, 1/200) diluted in TBS-Tween 20 0.1% for 2 h at room temperature. Two more washes followed by one in TBS without Tween 20 (5 min) were performed before the incubation with the red fluorophore, which is conjugated to tyramide signal amplification (TSA)-Cy3 activated by peroxidase (Perkin Elmer, 1/500). Finally, sections were washed and mounted with Mowiol.

The H_3R probe corresponded to nucleotides 636-1243 of the rat H_3R sequence. It was previously shown to hybridize to the various H_3R mRNA isoforms expressed in the brain or peripheral tissues [14,16]. The tyrosine hydroxylase probe used to detect dopaminergic neurons was complementary to rat tyrosine hydroxylase mRNA sequence from nucleotide 25 till the end. cDNAs for proenkephalin (PE) and SP were obtained by polymerase chain reaction and corresponded to nucleotides 335-641 (GenBank accession n° AH002996) and nucleotides 80 - 227 (AH002233), respectively. They were subcloned into pGEM-4Z (Promega) plasmids. Antisense and sense cRNA riboprobes were prepared by in vitro transcription. The sense probe was used as a control for the specificity of the signal obtained with the antisense probe.

Fluorescent immunohistochemistry

Brain sections were thawed at 4ºC, washed in TBS for 5 min, then in sodium borohydrate 1% (diluted in disodium hydrogenphosphate 0.1M pH 7.8) for 20 min and rinsed in phosphate buffer saline

50mM pH 7.4 and TBS (3 min each). Blocking was made with 7% donkey serum in TBS for 1 h at 37ºC. Primary antibodies (listed in **Table 1**) were diluted in buffer (TBS, acetylated bovine serum albumin 1%, Tween 20 0.1%, 7% donkey serum) and incubated overnight at 4ºC. Histamine H_3 receptor expression in dopaminergic and cholinergic neurons was detected using the Abcam antibody while the Alpha Diagnostic H3R31A antibody was employed for the other experiments as they showed similar immunostaining (Fig. 3). The H_3R signal specificity was tested by comparing three different commercial antibodies and by blocking Alpha Diagnostic anti-H_3 (H_3Ral) signal with its blocking peptide. After three washes in TBS-Tween 20 0.05%, sections were incubated with the secondary antibodies diluted in the same buffer as the primary. Specificity of the secondary antibodies employed was tested by control experiments without primary antibody. Three more washes with TBS-Tween 20 0.05% and TBS were done prior the incubation of 5 min with Hoechst33258 (diluted 1/1000 in TBS) for nuclei visualization. Final washes in TBS were made before the mounting with Mowiol.

Sections were analyzed with a Nikon Eclipse 90i microscope equipped with conventional fluorescence: (1) DAPI filters (340-380nm excitation, 435-485nm emission), (2) FITC filters (465-495nm excitation, 515-555nm emission) and (3) G2-A filters (510-560nm excitation, 590 emission). Fluorescent images were captured with a high resolution (1280x1024 pixels) Nikon digital DXM1200F camera interfaced with the ACT-1 Nikon software. Image signal levels were adjusted using Adobe Photoshop software for a better visualization. Original images have been kept. Confocal images are a Z-stack of 5 photos (1µm/slice) made with an Olympus FluoView FV1000 (Olympus) microscope equipped with a UPLSAPO 60x NA: 1.35 objective. The following lasers were used: a 488nm laser (488nm excitation, 520nm emission) and a 559nm laser (559nm excitation, 618nm emission). Since the intensity of immunolabelling for the antibodies used could be due to many variables that cannot be individually quantified, this study does not attempt to quantify the relative amounts of labelled antigens. Colocalization of both antigens were measured with the FV10-ASW 1.7 software (Olympus) and are shown as average overlap ± standard deviation of seven different regions of interest for each image. When the overlap value is above 0.5 we consider both antigens colocalized.

Electrophysiology

The protocol used was adapted from [29] and was as follows: Brains from male Sprague-Dawley rats of 5 - 9 weeks of age were rapidly extracted and placed in ice-cold Krebs buffer containing 124 mM NaCl, 3.5 mM KCl, 25 mM $NaHCO_3$, 1.25 mM NaH_2PO_4, 1 mM $CaCl_2$, 2 mM $MgSO_4$, 10 mM glucose, 10 mM Hepes (pH 7.4) and oxygen saturated (95% O_2/5% CO_2). Sagital corticostriatal slices (350 µm) were prepared from tissue blocks of the brain with a Vibratome (Leica, VT1000S) and maintained at least 2 h at room temperature in the Krebs buffer, containing 2 mM $CaCl_2$. This medium was used for further recordings. A single slice was transferred to a recording chamber of an upright microscope (DMLFS, Leica). The slice was positioned under a nylon mesh and continuously superfused with oxygen saturated Krebs solution (flow rate 2 ml/min) maintained at 30-32ºC. Extracellular recordings were made using a glass micropipette (flame polished borosilicate capillary, inside diameter 0.58 mm, outside diameter 1 mm, Warner instruments; resistance 4-7 MΩ) with a wire (silver, 250 µm, A-M Systems) filled with

perfusion medium and placed in the dorsal striatum. Afferent fibers were stimulated by delivering monophasic voltage pulses at a frequency of 0.05 Hz to a bipolar electrode (nickel chrome wire, bare diameter 50 µm, A-M Systems) connected to a multi-channel external stimulator (STG4, Multi channels systems) controlled by the software MC Stim (Multi channels systems). The stimulating electrode was placed in the corpus callosum, or in the striatum close to the border of the corpus callosum. Stimulation intensity ranged from 100-800 µA and 80-600 ms. The recording electrode was connected to a patch-clamp amplifier (Axopatch 200 B, Axon Instruments). Signals were digitized (Digidata 1200 Interface, Axon Instruments) and filtered at 2 kHz. Paired-pulse ratio was obtained by applying two stimuli with a 50 ms interval and calculated by dividing the second field potential amplitude by the amplitude of the first one (P2/P1). Data were collected by Win LTP (kind gift by Dr. W. Anderson, University of Bristol, UK). The amplitude of the field potential was used as a measure of synaptic transmission. After obtaining a stable baseline of at least 15 min, thioperamide was diluted in the Krebs solution and bath-applied. Field potential amplitudes were normalized to baseline amplitude. Each data point used for statistics was the mean of 8 consecutive field potentials. Results were pooled in Sigmaplot (Sigmaplot version 9) and represented as means (± SEM) of n= 5 animals.

Dopamine synthesis

Fresh rat brains were chilled immediately in modified Krebs-Ringer-bicarbonate medium with the following composition: 120 mM NaCl, 0.8 mM KCl, 2.6 mM $CaCl_2$, 0.67 mM $MgSO_4$, 1.2 mM KH_2PO_4, 27.5 mM $NaHCO_3$, and 10 mM glucose, pH 7.4, saturated with 95% O_2/5% CO_2. In a 4ºC room, striata (including nucleus accumbens) were dissected and sliced using a McIlwain tissue chopper to obtain miniprisms of 0.3-0.3 mm/side. Miniprisms were suspended in the same medium and washed by centrifugation and resuspension to remove cell debris. Miniprisims were distributed into 2 ml polypropylene tubes and preincubated for 15 min at 37ºC in an Eppendorf Thermomixer under 95% O_2/5% CO_2 atmosphere. Imetit (H_3R agonist) or vehicle was added and preincubation continued for 10 min. Then ring-labeled [3,5-^{3}H]-L-tyrosine (40–60 Ci/mmol) was added to all samples (final concentration of 0.12 µM) and incubation continued for 10 min to synthesize [^{3}H]-dopamine. Synthesis was stopped by the addition of a deproteinizing solution containing trichloroacetic acid and 100nmol internal standard dopamine per tube. Blank tubes contained deproteinizing solution prior to [^{3}H]-tyrosine and were kept ice-cold throughout. All samples were homogenized in a Dynatech/Sonic Dismembrator (Dynatech Labs). An aliquot was taken for protein quantification by the Lowry method to take into account the variability of tissue amounts in each tube. Tissue homogenates were then centrifuged (12,000 g, 10 min, 4ºC), and supernatants were recovered for [^{3}H]-dopamine purification by HPLC-UV.

The chromatography system consisted of a reverse-phase C18 column (Tracer Extrasil ODS2, 5-mm particle size, 25 x 0.46 cm; Teknokroma) and an ion-pair mobile phase, made up of 100 mM sodium phosphate buffer, 1 mM EDTA, 0,75 mM octanesulfonic acid plus 12% (v/v) methanol (pH 5). Flow rate was 1 ml/min. Internal standards were detected by UV 285 nm. Radiolabelled and endogenous tyrosine and dopamine were undetectable by UV absorbance. Recovery of the internal standard was quantified in each sample (internal/external standard peak area). Dopamine fractions were collected in

scintillation vials, mixed with Optiphase HiSafe III cocktail (Wallac), and [^{3}H]-dopamine was quantified in a liquid scintillation counter. Dpm obtained were corrected by dopamine internal standard recovery, dpm in blank samples, and protein content in each incubated tube. Results were expressed as percentage versus control samples in the same experiment.

Results

H_3R mRNA and protein expression in mesencephalic dopaminergic neurons.

In a previous study of H_3R mRNA distribution in several brain regions [16], no expression was apparent in the ventral tegmental area (VTA). In contrast in the present work we do describe H_3R mRNA expression in the VTA using the same H_3R cRNA probe for *in situ* hybridization as [16]. TSA amplification permitted to visualize H_3R expression, particularly in dopaminergic neurons of the VTA identified by tyrosine hydroxylase mRNA (double *in situ* hybridization) and protein (double immunohistochemistry; **Fig. 1A**). In agreement with Pillot et al [16] we confirm the presence of H_3R mRNA and protein in substantia nigra pars compacta (SNc, **Fig. 1B**), particularly in dopaminergic neurons. Additional neuronal populations of SNr also showed H_3R labeling (data not shown). The Pillot et al (2002) study also showed a low but significant binding of the H_3R ligand [^{125}I]-iodoproxyfan in the VTA as compared to the SNc. Thus, our results would agree with them after improvement of signal detection with TSA. Nevertheless, we controlled the specificity of the H_3 cRNA antisense probe used for *in situ* hybridization with the sense probe. In both our study and [16] a very low non-specific signal was detected in the VTA with the sense probe (**Fig. S1**), but it was almost undetectable when compared with the specific signal of the antisense probe in the same conditions. We also controlled the specificity of the H_3R antibodies used by comparing three different commercial antibodies (listed in **Table 1**) obtaining the same signal pattern. These antibodies where previously used in several studies [30,31]. Moreover, the signal specificity of the Alpha Diagnostic anti-H3R (anti-H3Ral) antibody was completely abolished by preincubation with its blocking peptide (**Fig. S2**)

H_3 receptors inhibit dopamine synthesis

Striatal dopamine synthesis takes place in dopaminergic terminals arising from VTA and SNc. To search for H_3R function in dopaminergic neurons we chose to determine dopamine synthesis in miniprism preparations of freshly dissected striatum. In the presence of different concentrations of the H_3R agonist imetit, [^{3}H]-dopamine synthesis from [^{3}H]-tyrosine was decreased by 65 % vs. controls ($p<0.01$ oneway ANOVA; **Fig. 2**). This result was representative of three independent experiments, and it confirms a previous report with a different H_3R agonist [9]. This suggests that H_3R are functional inhibitory heteroreceptors in dopaminergic neurons.

H_3R protein and mRNA expression in striatal neurons

Next we studied the presence of H_3R mRNA (**Fig. 3**) and protein (**Fig. 4**) in striatal GABAergic projection neurons. Approximately half of H_3R mRNA-positive neurons corresponded to each population of SP or PE-expressing GABAergic projection neurons **(Fig. 3)**. Almost all SP mRNA positive neurons expressed H_3R mRNA (111 double-labelled of 126 SP positive neurons in accumbens and 115 of 133 in striatum). Similarly, almost all PE mRNA positive neurons expressed H_3R mRNA (131 double-

labelled of 140 PE positive neurons in accumbens and 141 of 160 in striatum).

We also studied the colocalization of H_3R protein and dopamine D_1 receptor immunoreactivities. Dopamine D_1 receptor immunoreactivity was more intense in neuronal somas, although it showed a pattern of expression suggesting terminal labelling. Using confocal imaging, we found H_3R-D_1R colocalization (**Fig. 4**) in the H_3R positive neurons of the medial prefrontal cortex, dorsal striatum and nucleus accumbens (overlap values 0.71±0.01, 0.67±0.05 and 0.71±0.03 respectively) and also in H_3R positive terminals of these areas (overlap values 0.70±0.02, 0.70±0.03 and 0.74±0.04 respectively).

Although H_3R activation modulates acetylcholine release [32,33,34], the presence of H_3R on cholinergic neuron terminals had not yet been clearly established. We found H_3R immunoreactivity in virtually all accumbal (10 double-positive of 10 cholinergic neurons) and striatal (17 double-positive of 17 cholinergic neurons) cholinergic interneurons, as shown in **Fig. 5**. Cholinergic interneurons were identified by choline acetyltransferase (ChAT) immunoreactivity and by their big size.

H_3R protein expression in glutamatergic endings. Effects on glutamate release.

The striatum receives a modulatory histaminergic input arising from the tuberomammillary nucleus of the hypothalamus [35] and three major synaptic inputs: the dopaminergic nigrostriatal pathway and the glutamatergic corticostriatal and thalamostriatal pathways [36]. These two glutamatergic inputs to striatal neurons can be easily distinguished on the basis of the vesicular transporter used for glutamate storage. Thalamic neurons express the vesicular glutamate transporter 2 while cortical neurons innervating the striatum express the vesicular glutamate transporter 1 (VGLUT1) [37]. As **Fig. 6** shows, we found that H_3R are highly expressed in glutamatergic corticostriatal nerve endings (VGLUT1 immunoreactive) in striatum and nucleus accumbens (overlap values 0.75±0.08 and 0.72±0.04 respectively) as well as in glutamatergic terminals in the medial prefrontal cortex (overlap value 0.68±0.08). At the same time, we found H_3R-VGLUT1 colocalization in the external border of some H_3R positive neurons in medial prefrontal cortex, striatum and nucleus accumbens (overlap values 0.54±0.03, 0.60±0.03 and 0.62±0.05 respectively), while central area of the neurons only showed H_3R immunoreactivity.

To determine if H_3 receptors found on glutamatergic corticostriatal endings were functional, we recorded field potentials elicited by cortico-striatal stimulation. The application of H_3R antagonist/inverse agonist thioperamide (100 nM) to fresh striatal brain slices induced an increase of field potential amplitude accompanied by a decrease of the paired-pulse ratio (**Fig. 7**). This effect persisted during thioperamide application (30 min) and after washout ($p<0.05$ repeated-measures ANOVA), resulting in an enduring potentiation of field potential amplitude. A change in paired-pulse ratio is generally interpreted as a changed probability of neurotransmitter release reflecting a presynaptic action of the studied molecule. Thus the effects of 100 nM thioperamide clearly suggest a potentiation of corticostriatal glutamate release mediated by blockade of inhibitory H_3R present in corticostriatal nerve endings.

H_3R protein is not expressed in GFAP-immunoreactive astrocytes.

Astrocytes detected with an antibody against its specific marker, the glial fibrillary acidic protein (GFAP), are present

in diverse brain areas including the neostriatum, the substantia nigra and the cortex [38]. We analyzed the possible presence of H_3R in astrocytes and found no colocalization between H_3R and GFAP proteins in medial prefrontal cortex, striatum or nucleus accumbens (**Fig. 8).** Overlap values obtained in these three brain regions were 0.29±0.03, 0.26±0.07 and 0.27±0.07 respectively, always below the preestablished threshold to detect colocalization.

Discussion

In the present work we describe the presence of histamine H_3 receptor expression in several neuronal types of rat basal ganglia: (1) nigrostriatal and mesolimbic dopaminergic neurons; (2) striatonigral and striatopallidal GABAergic neurons; (3) striatal cholinergic interneurons and (4) corticostriatal glutamatergic terminals. In addition, we show that H_3 receptors appear to be functional in dopaminergic and glutamatergic cells. Thus H_3R are expressed in diverse cellular types and could mediate most histamine actions in these structures [39].

We describe for the first time H_3R mRNA presence in the VTA, which was not found in the study of brain H_3R distribution by Pillot *et al*. [16]. The reason for this discrepancy could be due to the sensitivity of methodological procedures. In the Pillot *et al*. work a ^{33}P radioactive probe was used for a one-week exposition time, a relatively short and probably insufficient period for low levels of mRNA expression. In our case we used the same cRNA probe as Pillot *et al*. but we detected it with the potent TSA amplification system. This improvement revealed H_3R mRNA expression in the VTA, specifically in dopaminergic cells. Pillot *et al*. also studied the brain distribution of H_3R protein by binding with the H_3R antagonist ^{125}I-iodoproxyfan. They found minimum binding in the VTA, much lower than in the dorsal striatum, Acb, cortex and substantia nigra (noteworthy weaker in SNc than in SNr, suggesting predominant H_3R expression in striatonigral neurons as compared to nigrostriatal neurons). Using fluorescent immunohistochemistry we have confirmed H_3R receptor presence in those areas (cortex, dorsal striatum, Acb, SNc and also VTA), but a comparison between regions was not attempted due to the difficulties of fluorescence quantification. Although H_3R expression can be lower in the VTA and SNc than in other regions, we show it is clearly present in dopaminergic neurons characterized both by tyrosine hydroxylase immunoreactivity and mRNA expression. Furthermore, H_3R stimulation decreased dopamine synthesis in striatal tissue (Fig. 2 and [9]), as expected according to the typically inhibitory role of H_3R in other cells [5,6]. Although dopamine release could also be modulated by H_3R, this effect was more clearly described in the prefrontal cortex than in the striatum [40,41]. In the Acb shell H_3R ligands modulate methamphetamine-stimulated dopamine release, but fail to modulate non-stimulated release [42]. Thus despite low expression levels, we can conclude that functional inhibitory H_3R are present in dopaminergic neurons projecting to the prefrontal cortex, dorsal striatum and Acb.

Colocalization of PE or SP mRNA with H_3R mRNA in the striatum and nucleus accumbens (Fig. 3) confirms H_3R expression in all GABAergic medium spiny projection neurons [43,44]. In striatonigral neurons, H_3R are functional taking into account that: 1) H_3R stimulation reduces dopamine D_1 receptor-dependent GABA release [11]; 2) H_3R stimulation inhibits dopamine D_1 receptor-stimulated cAMP accumulation

[45], and 3) D_1R - H_3R receptor heteromers stimulate MAP kinase specifically in these cells [44]. In striatopallidal neurons, H_3R presence agrees with 1) a previous report of H_3R mRNA in PE positive neurons [46] and 2) colocalization of D_2 and H_3 immunolabelling [44]. However, proof of H_3R functionality in striatopallidal neurons is still insufficient. D_2 and H_3 receptors can interact forming heteromers in living cells *in vitro*, and locomotor tests suggest they could also interact *in vivo* [46,47], but it is still uncertain whether this interaction actually occurs in striatal neurons [48]. Recently, Ellender *et al*. (2011) [39] reported that histamine modulates lateral inhibition between collaterals of striatal medium spiny neurons, although the authors did not test H_3R involvement in this effect.

Currently, the existence of a population of medium spiny neurons which coexpress D_1 and D_2 receptors is accepted [21,49]. In addition, all neurons expressing D_1 receptors appear to contain low levels of D_2 receptors and vice versa [20]. In the ventral striatum a subset of D_1 and D_2 receptor-expressing neurons coexpress dopamine D_3 receptors [50]. Additional populations of striatal efferent neurons coexpress (1) D_4 and D_5 receptors [51], (2) D_1 receptors, SP and also PE, projecting to the SNc [52], and (3) D_1 receptors and neurokinin B (but not SP or PE), projecting to the substantia innominata [19]. Thus, separation of neuronal populations can not be performed based on D_1 receptor labelling. In this paper all H_3R protein immunoreactive neurons in the studied areas showed D_1 protein immunoreactivity (Fig. 4). This might imply H_3R expression in neurons where D_1 and D_2 receptors are colocalized, but we did not attempt to demonstrate this by triple labelling. The specificity of the dopamine D_1 receptor antibody used here was described by Narushima *et al*. [53]. In Narushima's paper, partial colocalization of D_1 and D_2 receptor immunoreactivities was apparent in some pictures. Further work should confirm whether H_3R are expressed in D_1 - D_2 positive cells.

GABAergic and cholinergic interneuron arborizations in the caudate/putamen would explain neuropil colocalization between D_1 receptors and H_3R (Fig. 4). In contrast, glutamatergic inputs are described to express only the D_2-like class of dopamine receptors [54]. Similarly, the D_1R - H_3R protein colocalization found in the medial prefrontal cortex could be due to the H_3R presence in the D_1R-expressing GABAergic interneurons of the cortex.

It is well known that excitatory corticostriatal afferents to the striatum innervate both populations of medium-sized spiny GABAergic projection neurons [55]. We found H_3R immunoreactivity in corticostriatal glutamatergic inputs to the striatum (Fig. 6). The colocalization of H_3R and VGLUT1 agrees with functional studies showing that 1) the H_3R inverse agonist thioperamide at 100 nM changed the paired-pulse ratio of corticostriatal synapses (Fig. 7A), an index of altered probability of presynaptic neurotransmitter (glutamate) release [56]; 2) H_3R mediate the synaptic depression induced by histamine in corticostriatal inputs [57,39]. Conversely, the H_3R inverse agonist thioperamide relieves the repression exerted by presynaptic H_3R on glutamatergic terminals, allowing an increased release of presynaptic glutamate that potentiates field potentials (Fig. 7B). The concentration of thioperamide we used in the present study (100 nM) should fully occupy H_3R, although it is much lower than that used in Doreulee and Ellender studies (10 ?M) to block histamine-induced synaptic depression. We must note

that bath application of 10 ?M thioperamide alone did not affect field potential amplitude or paired pulse ratios (data confirmed by us, in agreement with previous studies [57, 39]). We do not have an explanation for thioperamide concentration-dependent effects, but we could speculate that higher concentrations may have effects on an additional subset of receptors (and see [13]). Independently of that, Ellender *et al*. (2011) [39] suggested that H_3R mediate histamine depression of corticostriatal synapses and favor thalamostriatal transmission, but the presence of H_3R in thalamostriatal terminals has not yet been demonstrated. H_3R activation in striatal synaptosomes inhibits glutamate release [10], but striatal synaptosomes may be formed from cortical, thalamic or additional inputs. Taken together, we can conclude that functionally inhibitory H_3R are present in corticostriatal terminals, limiting glutamate release.

Our results show that striatal cholinergic neurons present histamine H_3 receptor immunoreactivity. Due to the low number of striatal cholinergic interneurons, we were unable to show direct effects of H_3R ligands specifically in these cells, but there are numerous studies where H_3R modulation of acetylcholine release has been observed in diverse brain regions: (1) in the amygdala H_3R agonists increased acetylcholine release [58]; (2) in the cortex H_3R agonists decreased acetylcholine release [32,33]; (3) in the hippocampus H_3R antagonists increased acetylcholine release [59]; (4) in the ventral striatum of freely moving rats acetylcholine release was stimulated by both H_3R agonists and inverse agonists by acting at H_3 receptors putatively located in different populations of neurons, although no evidence was obtained of direct effects of H_3 ligands on cholinergic neurons [34]. Thus, the possibility that H_3 receptors in striatal cholinergic interneurons are functional is still uncertain.

Although we did not find H_3R presence in GFAP-immunoreactive astrocytes in the medial prefrontal cortex, striatum or nucleus accumbens, this colocalization was recently shown at the caudal spinal trigeminal nucleus of non-human primates [60]. Thus H_3R presence in astrocytes could be limited to some areas. In cultured astrocytes histamine seems to act through H_1 receptors to induce inositol phosphate accumulation [61] and calcium entry [62] but we have found no literature evidence of H_3 receptor-mediated effects in astrocytes.

Due to the presence of functional H_3R in such different cellular types, what role should these receptors have in striatal function? Regarding locomotion, it has been shown that histamine action on H_3R elicits a fast hypokinetic effect, and afterwards histamine would activate H_1 receptors to elicit hyperactivity [23]. The hypokinetic effect could be explained by a transient decrease of dopamine neurotransmission provoked by H_3R stimulation. However H_3R KO mice exhibit lower locomotion than wild-type mice [24], a finding that is hard to reconcile with the H_3-mediated hypokinetic effect and with the observation that H_3 antagonists do not change locomotor activity. An interpretation given by these authors is that the absence of H_3 inhibitory autoreceptors in histamine neurons of KO mice could favor histamine release, which could decrease neuronal histamine levels, which in turn could decrease activation of H_1 receptors [24]. Developmental adaptations in H_3R KO mice are difficult to interpret given the varied cellular types expressing H_3R in the basal ganglia.

Several H_3R agonists decrease L-dopa and apomorphine-induced turning

behavior in 6-hydroxydopamine lesioned rats [26,63] as well as L-dopa-induced chorea in MPTP-lesioned monkeys [28]. These effects could be due to H_3R-mediated decrease of GABA release in the SNr [64] (but see [65]). In reserpinized mice, H_3 receptor stimulation decreases locomotion induced by dopaminergic agonists [47]. These effects should be independent of H_3R expression in dopaminergic neurons. In brains from Parkinson disease patients a strong H_3R binding was found in the SNr [66]. Thus, it is likely that H_3R in the GABAergic direct pathway could account for the majority of the effects of H_3R agonists in models of Parkinson's disease. H_3R and D_1R in these neurons have opposite effects [11,44] and dopaminergic lesions may sensitize them [66,45].

The effects of H_3R antagonists / inverse agonists in the basal ganglia can be more difficult to interpret. H_3R inverse agonists would (1) stimulate histamine release, which may lead to H_1-mediated effects such as hyperlocomotion [23,67] and H_2-mediated depolarization of medium spiny neurons [39]; (2) facilitate glutamate release from corticostriatal terminals (Fig. 7); and (3) stimulate cortical dopamine release [40]. In reserpinized mice, the H_3R antagonists / inverse agonist thioperamide potentiates locomotion elicited by dopaminergic agonists [47]. However, antagonism of H_3R in striatonigral neurons could also block D_1-H_3 receptor heteromers [44], whose involvement in locomotion is uncertain, but could contribute to dopamine-mediated effects. D_1-H_3 receptor heteromers work as processors integrating dopaminergic and histaminergic signals that can be blocked by antagonists of either receptor protomer composing the heteromer [44]. According to H_3R expression in several neuronal types of the basal ganglia, further studies would be needed to determine whether H_3R ligands could be therapeutically useful in Parkinson's disease or related movement disorders [68]. Similarly, further studies of H_3R antagonists / inverse agonists would be advisable in models of other disorders where the basal ganglia play a central role such as attention-deficit hyperactivity disorder, schizophrenia and alcohol abuse [25,26]. The fact that each neuronal pathway involved expresses H_3R difficults prediction of the predominant functional effects of H_3R antagonists / inverse agonists. We expect these ligands would favor histamine actions on other histamine receptor subtypes, but their effects on glutamatergic and dopaminergic neurotransmissions must also be considered.

Ackowledgements

Supported by Spanish government grants SAF2006-08240, SAF2009-12510 and Red de Trastornos Adictivos RD06/0001/0015. M.G.S. was recipient of a Spanish government FPI fellowship. HH was recipient of an Allocation de Recherche from the French government.

References

[1]. Haas H, Panula P. The role of histamine and the tuberomamillary nucleus in the nervous system. Nat Rev Neurosci 2003; 4(2):121-30.

[2]. Yanai, K., & Tashiro, M. The physiological and pathophysiological roles of neuronal histamine: An insight from human positron emission tomography studies. Pharmacol Ther 2007; 113(1), 1-15.

[3]. Oda, T., Morikawa, N., Saito, Y., Masuho, Y., & Matsumoto, S. Molecular cloning and characterization of a novel type of histamine receptor preferentially expressed in leukocytes. J Biol Chem 2000; 275(47), 36781-6.

[4]. Connelly, W. M., Shenton, F. C., Lethbridge, N., Leurs, R., Waldvogel, H. J., Faull, R. L., et al. The histamine H4 receptor is functionally expressed on neurons in the mammalian CNS. Br J Pharmacol 2009; 157(1), 55-63.

[5]. Arrang, J. M., Garbarg, M., & Schwartz, J. C. Auto-inhibition of brain histamine release mediated by a novel class (H3) of histamine receptor. Nature 1983; 302(5911), 832-7.

[6]. Arrang, J. M., Garbarg, M., & Schwartz, J. C. Autoinhibition of histamine synthesis mediated by presynaptic H3-receptors. Neuroscience 1987; 23(1), 149-57.

[7]. Schlicker, E., Betz, R., & Gothert, M. Histamine H3 receptor-mediated inhibition of serotonin release in the rat brain cortex. Naunyn Schmiedebergs Arch Pharmacol 1988; 337(5), 588-90.

[8]. Schlicker, E., Fink, K., Hinterthaner, M., & Gothert, M. Inhibition of noradrenaline release in the rat brain cortex via presynaptic H3 receptors. Naunyn Schmiedebergs Arch Pharmacol 1989; 340(6), 633-8.

[9]. Molina-Hernandez, A., Nunez, A., & Arias-Montano, J. A. Histamine H3-receptor activation inhibits dopamine synthesis in rat striatum. Neuroreport 2000; 11(1), 163-6.

[10]. Molina-Hernandez, A., Nunez, A., Sierra, J. J., & Arias-Montano, J. A. Histamine H3 receptor activation inhibits glutamate release from rat striatal synaptosomes. Neuropharmacology 2001; 41(8), 928-34.

[11]. Arias-Montano, J. A., Floran, B., Garcia, M., Aceves, J., & Young, J. M. Histamine H(3) receptor-mediated inhibition of depolarization-induced, dopamine D(1) receptor-dependent release of [(3)H]-gamma-aminobutryic acid from rat striatal slices. Br J Pharmacol 2001; 133(1), 165-71.

[12]. Esbenshade TA, Browman KE, Bitner RS, Strakhova M, Cowart MD, Brioni JD. The histamine H3 receptor: an attractive target for the treatment of cognitive disorders. Br J Pharmacol 2008; 154(6):1166-81.

[13]. Gbahou F, Rouleau A, Arrang JM. The histamine autoreceptor is a short isoform of the H(3) receptor. Br J Pharmacol 2012; 166(6):1860-71.

[14]. Morisset, S., Sasse, A., Gbahou, F., Heron, A., Ligneau, X., Tardivel-Lacombe, J., et al.. The rat H3 receptor: Gene organization and multiple isoforms. Biochem Biophys Res Commun 2001; 280(1), 75-80.

[15]. Lovenberg, T. W., Roland, B. L., Wilson, S. J., Jiang, X., Pyati, J., Huvar, A., et al. Cloning and functional expression of the human histamine H3 receptor. Mol Pharmacol 1999; 55(6), 1101-7.

[16]. Pillot, C., Heron, A., Cochois, V., Tardivel-Lacombe, J., Ligneau, X., Schwartz, J. C., et al. A detailed mapping of the histamine H(3) receptor and its gene transcripts in rat brain. Neuroscience 2002; 114(1), 173-93.

[17]. Morgane, P. J., Galler, J. R., & Mokler, D. J. A review of systems and networks of the limbic forebrain/limbic midbrain. Prog. Neurobiol 2005; 75(2), 143-160.

[18]. Le Moine, C., & Bloch, B. D1 and D2 dopamine receptor gene expression in the rat striatum: Sensitive cRNA probes demonstrate prominent segregation of D1 and D2 mRNAs in distinct neuronal populations of the dorsal and ventral striatum. J Comp Neurol 1995; 355(3), 418-26.

[19]. Sonomura, T., Nakamura, K., Furuta, T., Hioki, H., Nishi, A., Yamanaka, A., et al. Expression of D1 but not D2 dopamine receptors in striatal neurons producing neurokinin B in rats. Eur J Neurosci 2007; 26(11), 3093-103.

[20]. Aizman, O., Brismar, H., Uhlen, P., Zettergren, E., Levey, A. I., Forssberg, H., et al. Anatomical and physiological evidence for D1 and D2 dopamine receptor colocalization in neostriatal neurons. Nat Neurosci 2000; 3(3), 226-30.

[21]. Valjent, E., Bertran-Gonzalez, J., Herve, D., Fisone, G., & Girault, J. A. Looking BAC at striatal signaling: Cell-specific analysis in new transgenic mice. Trends Neurosci 2009; 32(10), 538-47.

[22]. Kawaguchi, Y. Neostriatal cell subtypes and their functional roles. Neurosci Res 1997; 27(1), 1-8.

[23]. Chiavegatto, S., Nasello, A. G., & Bernardi, M. M. Histamine and spontaneous motor activity: Biphasic changes, receptors involved and participation of the striatal dopamine system. Life Sci 1998; 62(20), 1875-88.

[24]. Toyota, H., Dugovic, C., Koehl, M., Laposky, A. D., Weber, C., Ngo, K., et al. Behavioral characterization of mice lacking histamine H(3) receptors. Mol Pharmacol 2002; 62(2), 389-97.

[25]. Passani MB, Blandina P. Histamine receptors in the CNS as targets for therapeutic intervention. Trends Pharmacol Sci. 2011;32(4):242-9.

[26]. Kuhne S, Wijtmans M, Lim HD, Leurs R, de Esch IJ. Several down, a few to go: histamine H3 receptor ligands making the final push towards the market? Expert Opin Investig Drugs. 2011;20(12):1629-48

[27]. Huotari, M., Kukkonen, K., Liikka, N., Potasev, T., Raasmaja, A., & Mannisto, P. T. Effects of histamine H(3)-ligands on the levodopa-induced turning behavior of hemiparkinsonian rats. Parkinsonism Relat Disord 2000; 6(3), 159-64.

[28]. Gomez-Ramirez, J., Johnston, T. H., Visanji, N. P., Fox, S. H., & Brotchie, J. M. Histamine H3 receptor agonists reduce L-dopa-induced chorea, but not dystonia, in the MPTP-lesioned nonhuman primate model of parkinson's disease. Mov Disord 2006; 21(6), 839-46.

[29]. Lante, F., de Jesus Ferreira, M. C., Guiramand, J., Recasens, M., & Vignes, M. Low-frequency stimulation induces a new form of LTP, metabotropic glutamate (mGlu5) receptor- and PKA-dependent, in the CA1 area of the rat hippocampus. Hippocampus 2006; 16(4), 345-60.

[30]. Lazarov, N. E., Reindl, S., Fischer, F., & Gratzl, M. Histaminergic and dopaminergic traits in the human carotid body. Respir Physiol Neuro 2009; 165(2-3), 131-6.

[31]. Karlstedt, K., Ahman, M. J., Anichtchik, O. V., Soinila, S., & Panula, P. Expression of the H3 receptor in the developing CNS and brown fat suggests novel roles for histamine. Mol Cell Neurosci 2003; 24(3), 614-22.

[32]. Clapham, J., & Kilpatrick, G. J. Histamine H3 receptors modulate the release of [^{3}H]-acetylcholine from slices of rat entorhinal cortex: Evidence for the possible existence of H3 receptor subtypes. Br J Pharmacol 1992; 107(4), 919-23.

[33]. Arrang, J. M., Drutel, G., & Schwartz, J. C. Characterization of histamine H3 receptors regulating acetylcholine release in rat entorhinal cortex. Br J Pharmacol 1995; 114(7), 1518-22.

[34]. Prast, H., Tran, M. H., Fischer, H., Kraus, M., Lamberti, C., Grass, K., et al. Histaminergic neurons modulate acetylcholine release in the ventral striatum: Role of H3 histamine receptors. Naunyn Schmiedebergs Arch Pharmacol 1999; 360(5), 558-64.

[35]. Panula, P., Flugge, G., Fuchs, E., Pirvola, U., Auvinen, S., & Airaksinen, M. S. Histamine-immunoreactive nerve fibers in the mammalian spinal cord. Brain Res 1989; 484(1-2), 234-9.

[36]. Smith, Y., Raju, D. V., Pare, J. F., & Sidibe, M. The thalamostriatal system: A highly specific network of the basal ganglia circuitry. Trends Neurosci 2004; 27(9), 520-527.

[37]. Kaneko, T., & Fujiyama, F. Complementary distribution of vesicular glutamate transporters in the central nervous system. Neurosci Res 2002; 42(4), 243-50.

[38]. Savchenko, V. L., McKanna, J. A., Nikonenko, I. R., & Skibo, G. G. Microglia and astrocytes in the adult rat brain: Comparative immunocytochemical analysis demonstrates the efficacy of lipocortin 1 immunoreactivity. Neuroscience 2000; 96(1), 195-203.

[39]. Ellender TJ, Huerta-Ocampo I, Deisseroth K, Capogna M, Bolam JP. Differential modulation of excitatory and inhibitory striatal synaptic transmission by histamine. J Neurosci 2011; 31(43):15340-51.

[40]. Ligneau, X., Perrin, D., Landais, L., Camelin, J. C., Calmels, T. P., Berrebi-Bertrand, I., et al. BF2.649 [1-{3-[3-(4-chlorophenyl)propoxy]propyl}piperidine, hydrochloride], a nonimidazole inverse agonist/antagonist at the human histamine H3 receptor: Preclinical pharmacology. J Pharmacol Exp Ther 2007; 320(1), 365-75.

[41]. Schlicker, E., Fink, K., Detzner, M., & Gothert, M. Histamine inhibits dopamine release in the mouse striatum via presynaptic H3 receptors. J Neural Transm Gen Sect 1993; 93(1), 1-10.

[42]. Munzar, P., Tanda, G., Justinova, Z., & Goldberg, S. R. Histamine H3 receptor antagonists potentiate methamphetamine self-administration and methamphetamine-induced accumbal dopamine release. Neuropsychopharmacology 2004; 29(4), 705-17.

[43]. Ryu, J. H., Yanai, K., Iwata, R., Ido, T., & Watanabe, T. Heterogeneous distributions of histamine H_3, dopamine D_1 and D_2 receptors in rat brain. Neuroreport 1994; 5(5), 621-4.

[44]. Moreno, E., Hoffmann, H., Gonzalez-Sepulveda, M., Navarro, G., Casado, V., Cortes, A., et al. Dopamine D1-histamine H3 receptor heteromers provide a selective link to MAPK signaling in GABAergic neurons of the direct striatal pathway. J Biol Chem 2011; 286(7), 5846-54.

[45]. Sanchez-Lemus, E., & Arias-Montano, J. A. Histamine H_3 receptor activation inhibits dopamine D1 receptor-induced cAMP accumulation in rat striatal slices. Neurosci Lett 2004; 364(3), 179-84.

[46]. Pillot, C., Ortiz, J., Heron, A., Ridray, S., Schwartz, J. C., & Arrang, J. M. Ciproxifan, a histamine H3-receptor antagonist/inverse agonist, potentiates neurochemical and behavioral effects of haloperidol in the rat. J Neurosci 2002 ; 22(16), 7272-80.

[47]. Ferrada, C., Ferre, S., Casado, V., Cortes, A., Justinova, Z., Barnes, C., et al. Interactions between histamine H(3) and dopamine D(2) receptors and the implications for striatal function. Neuropharmacology 2008; 55(2), 190-7.

[48]. Humbert-Claude, M., Morisset, S., Gbahou, F., & Arrang, J. M. Histamine H3 and dopamine D2 receptor-mediated [35S]GTPgamma[S] binding in rat striatum: Evidence for additive effects but lack of interactions. Biochem Pharmacol 2007 ; 73(8), 1172-81.

[49]. Perreault, M. L., Hasbi, A., Alijaniaram, M., Fan, T., Varghese, G., Fletcher, P. J., et al. The dopamine D1-D2 receptor heteromer localizes in dynorphin/enkephalin neurons: Increased high affinity state following amphetamine and in schizophrenia. J Biol Chem 2010; 285(47), 36625-36634.

[50]. Le Moine, C., & Bloch, B. Expression of the D3 dopamine receptor in peptidergic neurons of the nucleus accumbens: Comparison with the D1 and D2 dopamine receptors. Neuroscience 1996; 73(1), 131-43.

[51]. Smith, Y., & Kieval, J. Z. Anatomy of the dopamine system in the basal ganglia. Trends Neurosci 2000; 23(10 Suppl), S28-33.

[52]. Wang, H. B., Deng, Y. P., & Reiner, A. In situ hybridization histochemical and immunohistochemical evidence that striatal projection neurons co-containing substance P and enkephalin are overrepresented in the striosomal compartment of striatum in rats. Neurosci Lett 2007; 425(3), 195-9.

[53]. Narushima, M., Uchigashima, M., Hashimoto, K., Watanabe, M., & Kano, M. Depolarization-induced suppression of inhibition mediated by endocannabinoids at synapses from fast-spiking interneurons to medium spiny neurons in the striatum. Eur J Neurosci 2006; 24(8), 2246-52.

[54]. David, H. N., Ansseau, M., & Abraini, J. H. Dopamine-glutamate reciprocal modulation of release and motor responses in the rat caudate-putamen and nucleus accumbens of "intact" animals. Brain Research. Brain Res Rev 2005; 50(2), 336-360.

[55]. Lei, W., Jiao, Y., Del Mar, N., & Reiner, A. Evidence for differential cortical input to direct pathway versus indirect pathway striatal projection neurons in rats. J Neurosci 2004; 24(38), 8289-99.

[56]. Thomson, A. M. Facilitation, augmentation and potentiation at central synapses. Trends in Neuroscience 2000; 23(7), 305-12.

[57]. Doreulee, N., Yanovsky, Y., Flagmeyer, I., Stevens, D. R., Haas, H. L., & Brown, R. E. Histamine H(3) receptors depress synaptic transmission in the corticostriatal pathway. Neuropharmacology 2001; 40(1), 106-13.

[58]. Cangioli, I., Baldi, E., Mannaioni, P. F., Bucherelli, C., Blandina, P., & Passani, M. B. Activation of histaminergic H3 receptors in the rat basolateral amygdala improves expression of fear memory and enhances acetylcholine release. Eur J Neurosci 2002; 16(3), 521-8.

[59]. Bacciottini, L., Passani, M. B., Giovannelli, L., Cangioli, I., Mannaioni, P. F., Schunack, W., et al. Endogenous histamine in the medial septum-diagonal band complex increases the

release of acetylcholine from the hippocampus: A dual-probe microdialysis study in the freely moving rat. Eur J Neurosci 2002; 15(10), 1669-80.

[60]. Sekizawa, S., Bechtold, A. G., Tham, R. C., Kott, K. S., Hyde, D. M., Joad, J. P., et al. House-dust mite allergen and ozone exposure decreases histamine H3 receptors in the brainstem respiratory nuclei. Toxicol Appl Pharmacol 2010; 247(3), 204-10.

[61]. Kondou, H., Inagaki, N., Fukui, H., Koyama, Y., Kanamura, A., & Wada, H. Histamine-induced inositol phosphate accumulation in type-2 astrocytes. Biochem Biophys Res Commun 1991; 177(2), 734-8.

[62]. Jung, S., Pfeiffer, F., & Deitmer, J. W. Histamine-induced calcium entry in rat cerebellar astrocytes: Evidence for capacitative and non-capacitative mechanisms. J Physiol 2000; 527 Pt 3, 549-61.

[63]. Liu, C. Q., Hu, D. N., Liu, F. X., Chen, Z., & Luo, J. H. Apomorphine-induced turning behavior in 6-hydroxydopamine lesioned rats is increased by histidine and decreased by histidine decarboxylase, histamine H1 and H2 receptor antagonists, and an H3 receptor agonist. Pharmacol Biochem Behav 2008; 90(3), 325-30.

[64]. Garcia-Ramirez, M., Aceves, J., & Arias-Montano, J. A. Intranigral injection of the H3 agonist immepip and systemic apomorphine elicit ipsilateral turning behaviour in naive rats, but reduce contralateral turning in hemiparkinsonian rats. Behav Brain Res 2004; 154(2), 409-15.

[65]. Yanovsky Y, Li S, Klyuch BP, Yao Q, Blandina P, Passani MB, et al. L-Dopa activates histaminergic neurons. J Physiol 2011; 589(Pt 6):1349-66

[66]. Anichtchik, O. V., Peitsaro, N., Rinne, J. O., Kalimo, H., & Panula, P. Distribution and modulation of histamine H(3) receptors in basal ganglia and frontal cortex of healthy controls and patients with parkinson's disease. Neurobiology of Disease 2001; 8(4), 707-16.

[67]. Zhou, F. W., Xu, J. J., Zhao, Y., LeDoux, M. S., & Zhou, F. M. Opposite functions of histamine H1 and H2 receptors and H3 receptor in substantia nigra pars reticulata. J Neurophysiol 2006; 96(3), 1581-91.

[68]. Ercan-Sencicek AG, Stillman AA, Ghosh AK, Bilguvar K, O'Roak BJ, Mason CE, et al. L-histidine decarboxylase and Tourette's syndrome. N Engl J Med 2010; 362(20):1901-8.

Table 1. List of antibodies (A) **and fluorescent detection systems** (B) used for immunofluorescence and fluorescent *in situ* hybridization studies. Histamine H_3 receptor protein was detected using the Abcam 13014 antibody in dopaminergic and cholinergic neurons and the Alpha Diagnostic H3R31A antibody in the rest of experiments.

A

Antigen	Abbreviation	Dilution	Reference	Host
Histamine H_3 receptor	anti-H_3Rab	1/300	Abcam (ab-13014)	Rabbit (P)
Histamine H_3 receptor	anti-H_3Rc	1/200	Chemicon (ab5660)	Rabbit (P)
Histamine H_3 receptor	anti-H_3Ral	1/200	Alpha Diagnostic (H3R31-A)	Rabbit (P)
Tyrosine Hydroxylase	anti-TH	1/500	Millipore (AB1542)	Sheep (P)
Dopamine D1 receptor	anti-D1	1/300	Frontier Institute (D1rgpaf501)	G. Pig (P)
Choline Acetyl Transferase	anti-ChAT	1/100	Chemicon (ab144P)	Goat (P)
Vesicular Glutamate Transporter 1	anti-VGLUT1	1/300	Synaptic Systems (135 511)	Mouse (M)
Glial fibrillary Acidic Protein	anti-GFAP	1/500	Sigma Aldrich (G3893)	Mouse (M)

P, polyclonal; M, monoclonal

B

Detection system	Dilution	Source	Host
Anti Digoxigenin -peroxidase	1/100	Roche (11207733910)	Sheep
Anti-rabbit-peroxidase	1/200	Cell signalling (7074)	Goat
Anti biotine	1/200	Jackson Immun. (200-002-211)	Mouse
Anti mouse -Alexa 488	1/200	Invitrogen (A11029)	Goat
Anti sheep -FITC	1/40	Sigma Aldrich (F7634)	Donkey
Anti goat -Alexa 488	1/200	Invitrogen (A11055)	Donkey
Anti guinea pig -Alexa 488	1/200	Invitrogen (A11073)	Goat
Anti rabbit –Alexa594	1/200	Invitrogen (A21442)	Chicken
TSA-Cy3 (amplification system)	1/100-500	Perkin Elmer (NEL 744)	-
Hoechst 33258	1/10000	Invitrogen (H3569)	-

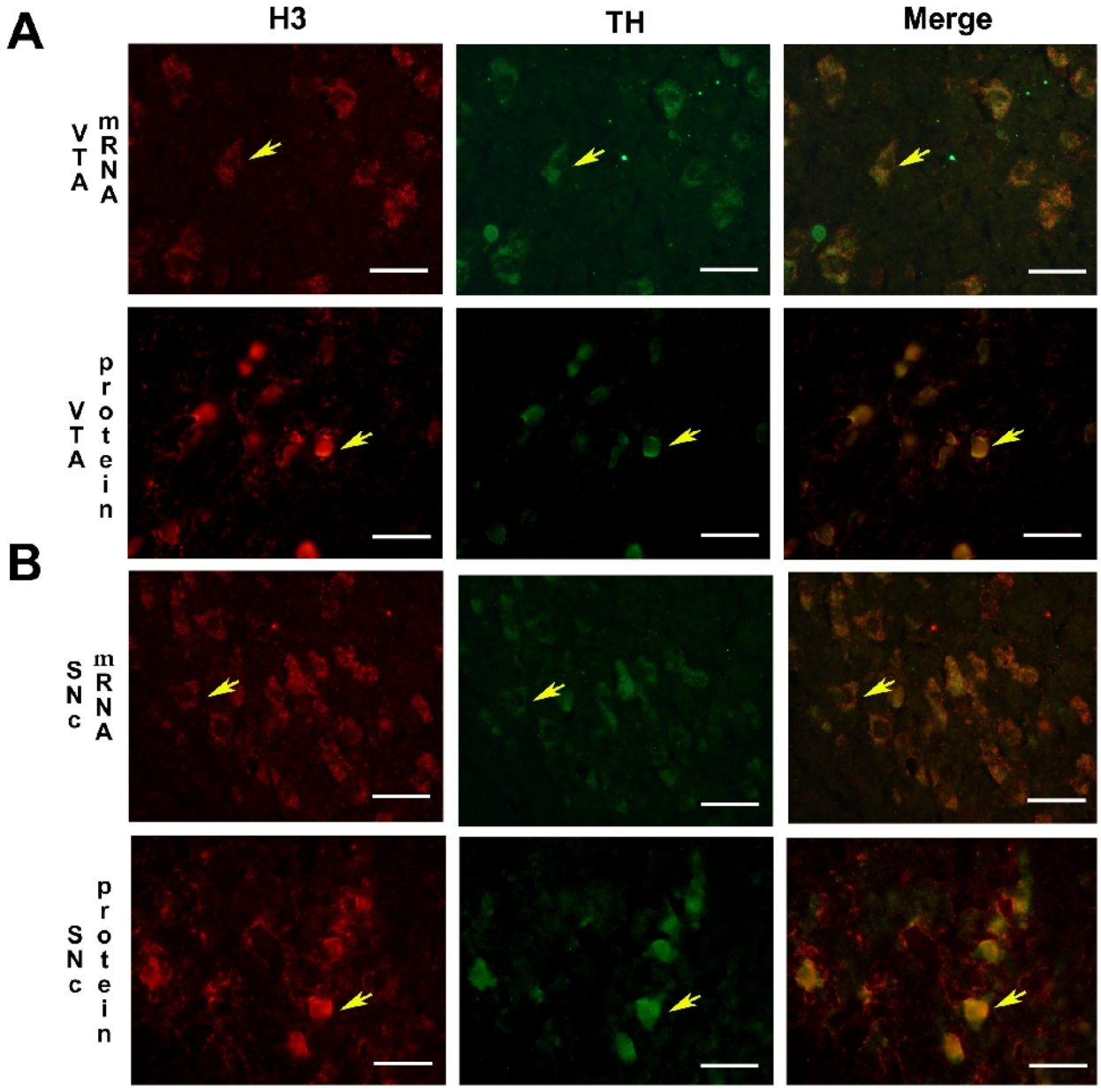

Figure 1. H_3R expression in mesencephalic dopamine neurons. A) Representative colocalization of H_3R and TH mRNAs (upper images) and protein immunoreactivities (lower images) in the VTA (scale bar 40µm). B) Colocalization of H_3R and TH mRNAs (upper images) and protein immunoreactivities (lower images) in the SNc (scale bar, 40µm). Images are representative of three brain sections obtained from different animals. H_3R protein immunoreactivity is detected with the Abcam rabbit anti-H_3R antibody and an anti-rabbit secondary coupled to DIG. H_3R mRNA is detected with a H_3R-specific cRNA-DIG probe. In both protocols, an anti-DIG-peroxidase antibody is used followed by TSA-Cy3 signal amplification, which gives a red labelling to H_3R expressing cells. TH protein is detected with a sheep anti-TH antibody and an anti-sheep FITC-coupled secondary antibody. TH mRNA is detected with a cRNA-biotin probe, followed by a mouse anti-biotin antibody and an anti-mouse Alexa 488-coupled antibody. In both cases a green label shows TH-expressing cells. Yellow arrows show neurons with positive colocalization.

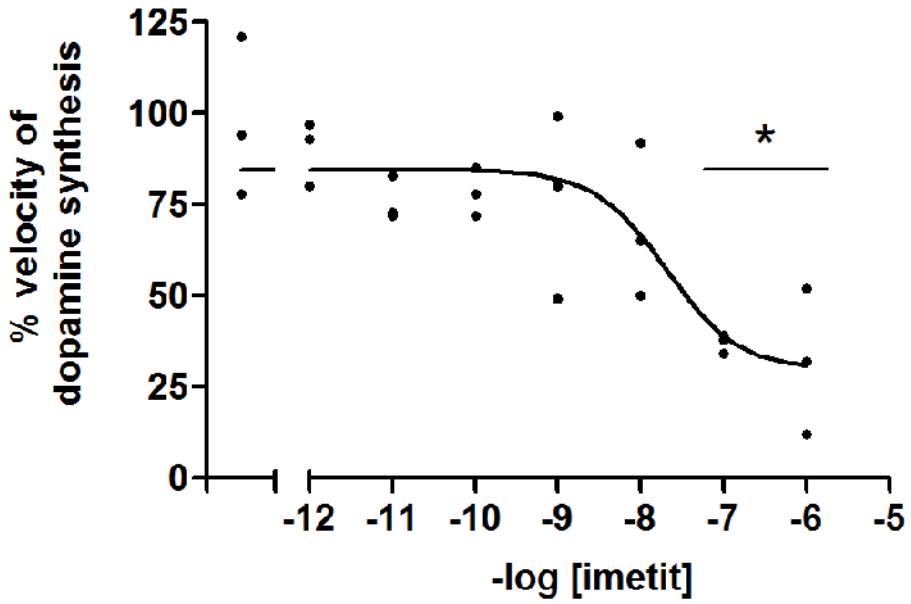

Figure 2. Inhibition of dopamine synthesis by a H_3R agonist. The H_3R agonist imetit dose-dependently decreased ^{3}H-dopamine synthesis in fresh striatal miniprisms incubated with ^{3}H-tyrosine. Data shown are obtained from individual incubations and expressed as % of dopamine synthesis versus control samples. 100% dopamine synthesis in control samples was 162667 dpm. This result was representative of three independent experiments performed with brains obtained from three different animals. Estimated IC_{50} was 20 nM. * $p<0.01$ vs controls, one-way ANOVA and Dunnett post-hoc test.

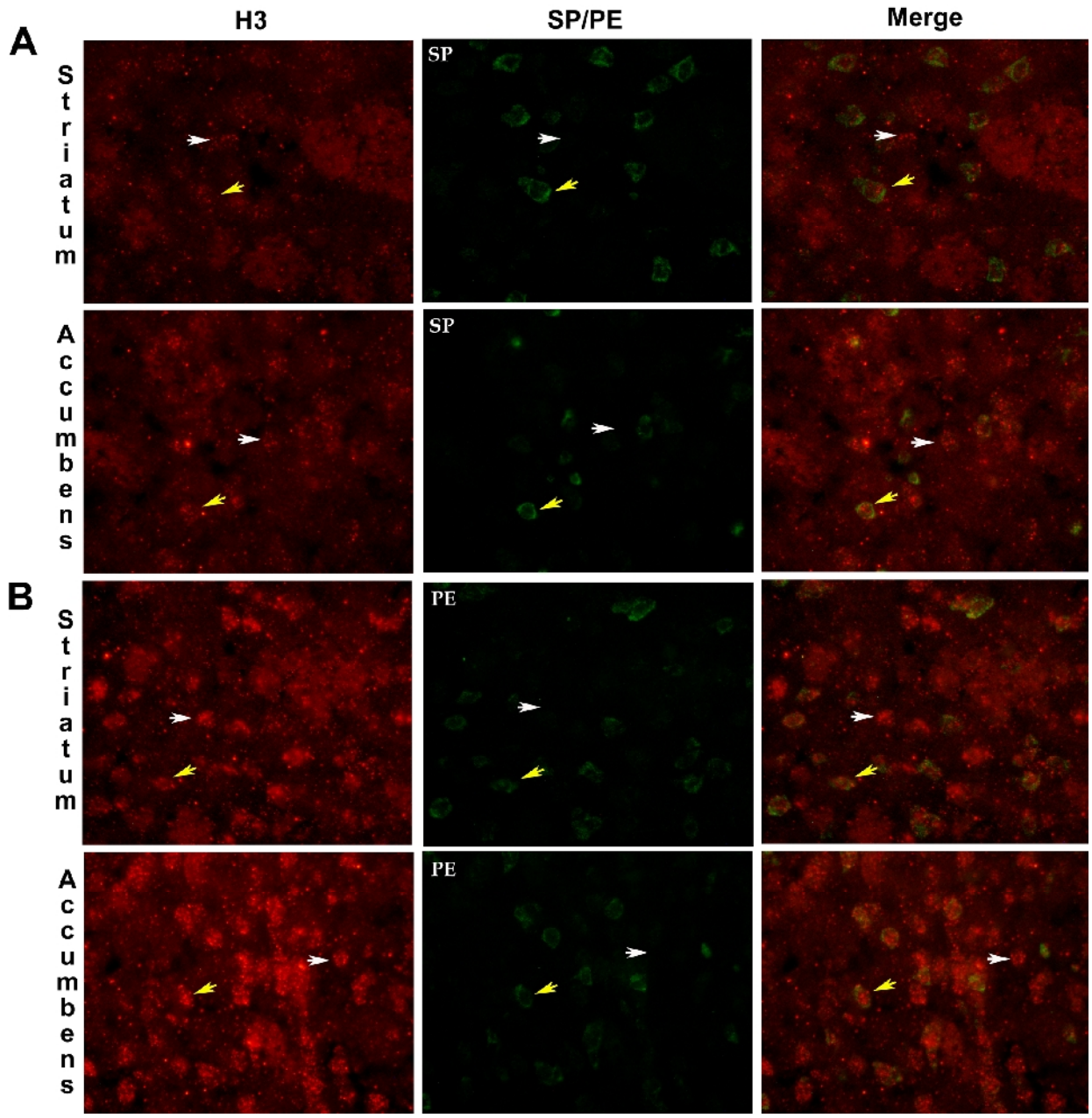

Figure 3. H_3R mRNA expression in GABAergic medium spiny projection neurons of the striatum and nucleus accumbens. A) H_3R mRNA colocalization with SP mRNA B) H_3R mRNA colocalization with PE mRNA. Images are representative of three brain sections obtained from different animals. H_3R mRNA is detected as a red fluorescent signal obtained using a H_3R-specific cRNA-DIG probe recognized by an anti-DIG-peroxidase antibody and followed by a TSA-Cy3 signal amplification. PE or SP mRNAs are detected as green fluorescence signals obtained using PE or SP cRNA-Biotin probes recognized by a mouse Anti-biotin antibody and followed by a goat anti-mouse Alexa 488-coupled antibody. White arrows show neurons single-labelled with H_3R mRNA only. Yellow arrows show positive neurons for both probes. Scale bar 40µm.

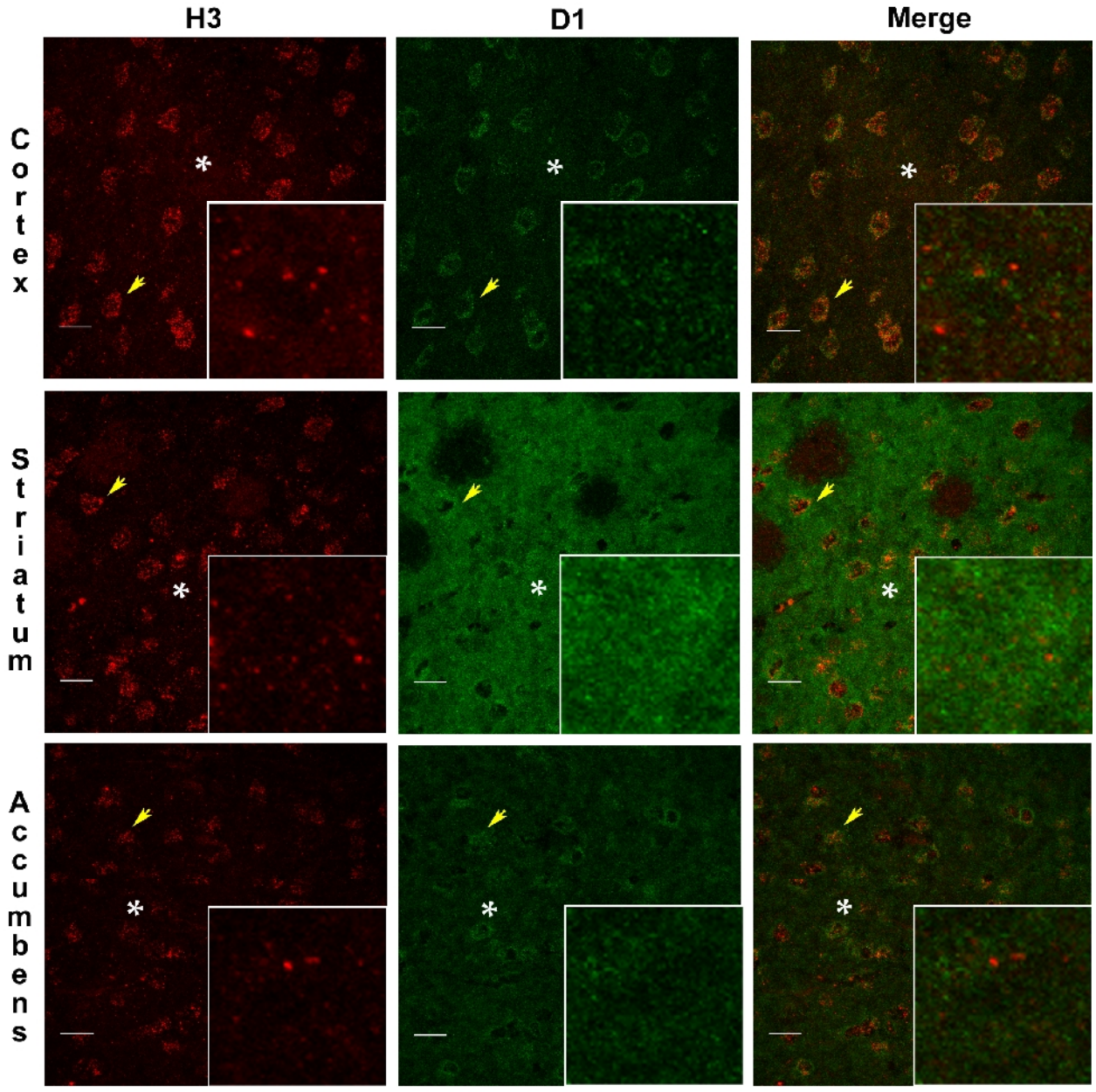

Figure 4. Colocalization of H_3R and D_1R immunoreactivities. H_3R and D_1R protein immunolabelling colocalize at neuronal bodies of the medial prefrontal cortex, dorsal striatum and nucleus accumbens (overlap values 0.71±0.01, 0.67±0.05 and 0.71±0.03 respectively) and neuropil of these areas (overlap values 0.70±0.02, 0.70±0.03 and 0.74±0.04 respectively. No neurons were found with only H_3R immunoreactivity. Images are representative of three brain sections obtained from different animals. H_3R protein is detected as red fluorescence obtained with the Alpha Diagnostic rabbit anti-H_3R antibody followed by an anti-rabbit-peroxidase and the TSA-Cy3 system. D_1 protein is detected as green fluorescence obtained with the guinea pig anti-D_1 antibody followed by the goat anti-guinea pig-Alexa488 antibody. Yellow arrows show positive neurons for both antibodies. Asterisks mark colocalization of immunoreactivity at nerve terminals. The insert show a zoom (7x) of the area marked by the asterisk. Scale bar 20µm.

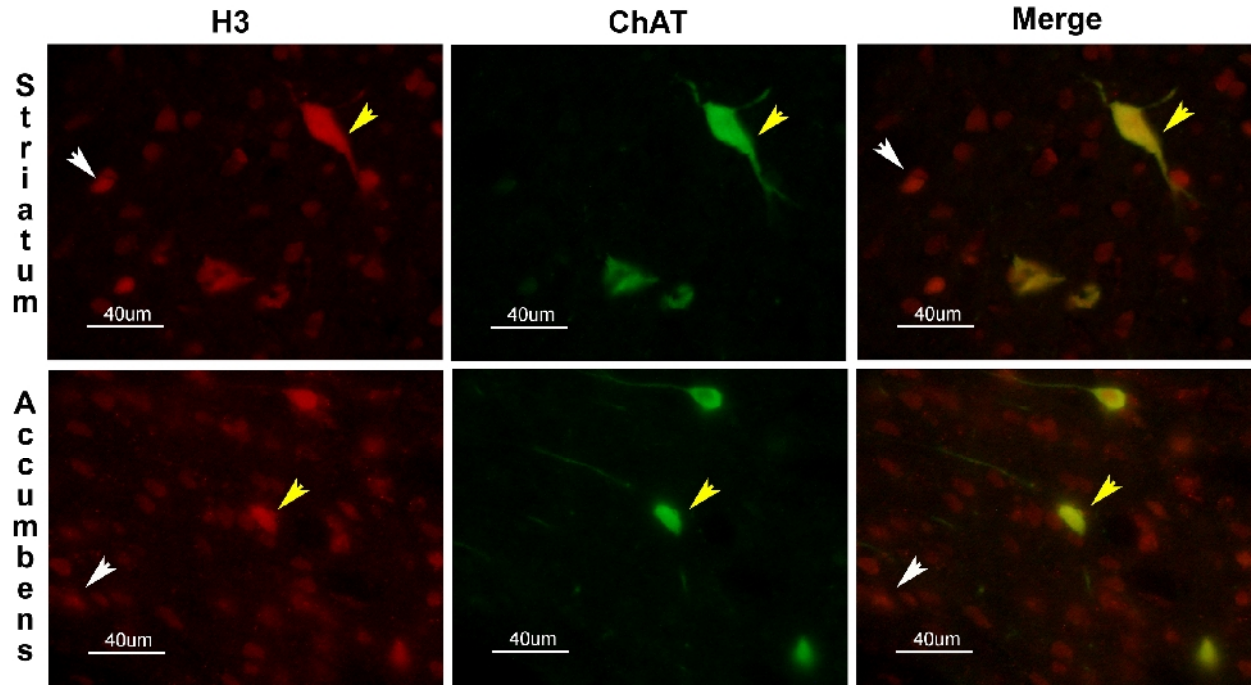

Figure 5. Presence of H_3R immunoreactivity in cholinergic (ChAT-immunoreactive) neurons in striatum and nucleus accumbens. ChAT immunoreactivity is found in big size H_3R-immunoreactive neurons. H_3R positive – ChAT negative neurons are also found. Images are representative of three different brain sections obtained from three animals. H_3R protein is detected as red fluorescence obtained with the Abcam rabbit anti-H_3R antibody developed with a chicken anti-rabbit-Alexa594 antibody. ChAT protein is detected as green fluorescence obtained by the goat anti-ChAT antibody developed with the donkey anti-goat-Alexa488 antibody. White arrows show neurons with H_3R protein immunoreactivity only. Yellow arrows show colocalization of both antibodies. Scale bar 40µm

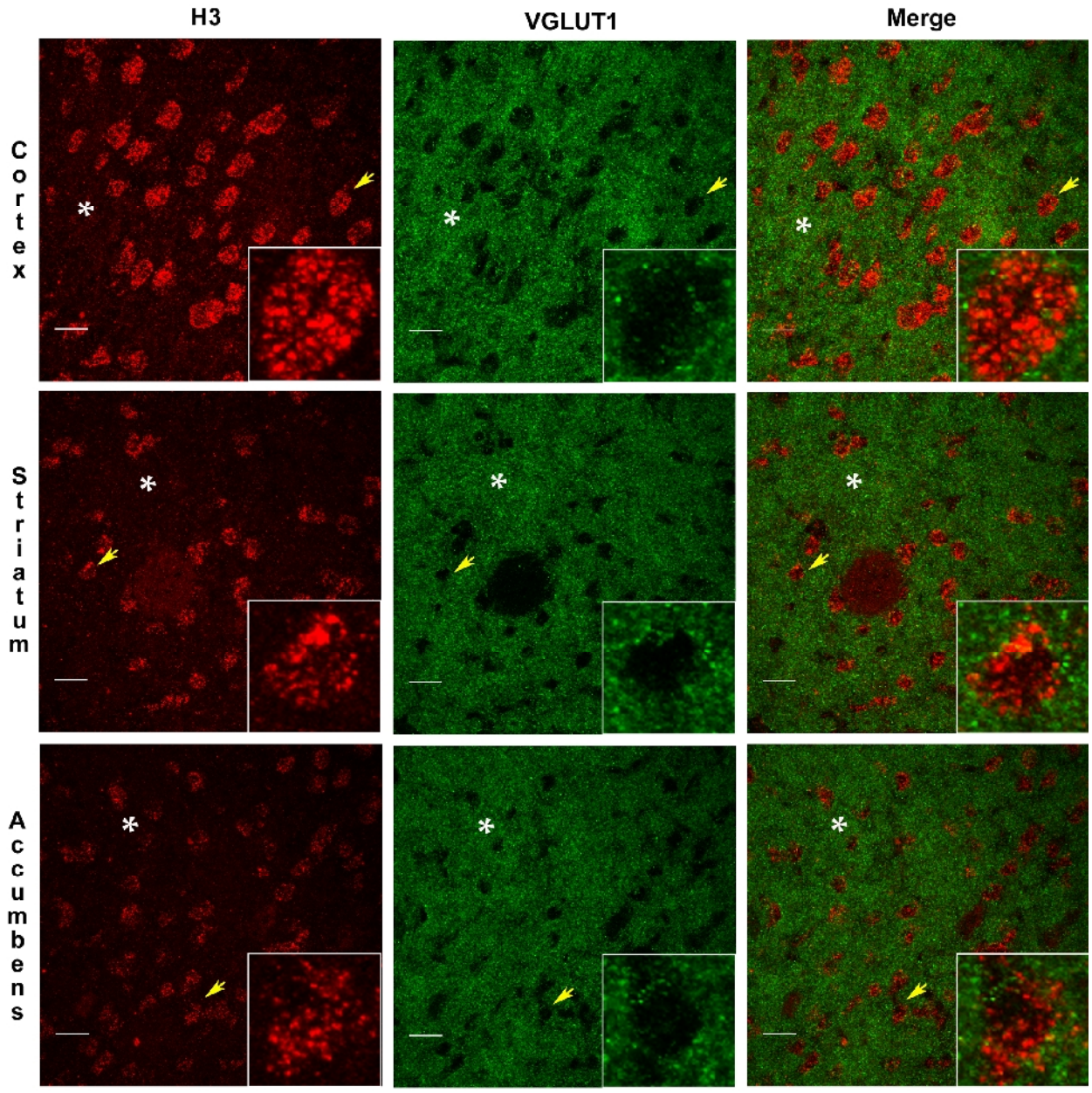

Figure 6. Presence of glutamatergic (VGLUT1-immunoreactive) terminals surrounding H_3R immunoreactive neurons. There is a clear terminal-axon (neuropil) VGLUT1 pattern of expression that spares most H_3R labelling located in the cell bodies. Colocalization between H_3R and VGLUT1 can be found in the neuropil of the medial prefrontal cortex, striatum and nucleus accumbens (overlap values 0.68±0.08, 0.75±0.08 and 0.72±0.04 respectively) and in the external border of some H_3R immunoreactive neurons (overlap values 0.54±0.03, 0.60±0.03 and 0.62±0.05 respectively in the same regions). Images are representative of three brain sections obtained from different animals. H_3R protein is detected as red fluorescence obtained with the Alpha Diagnostic rabbit anti-H_3R antibody followed by an anti-rabbit-peroxidase and the TSA-Cy3 system. VGLUT1 protein is detected as green fluorescence by the mouse anti-VGLUT1 antibody developed with the goat anti-mouse-Alexa488 antibody. Yellow arrows show positive neurons for both antibodies while asterisks mark immunoreactive colocalization at terminals. The insert shows a zoom (5x) of the neurons marked with a yellow arrow, where VGLUT1 protein is detected in the external border of H_3R immunoreactive neurons. Bar 20µm.

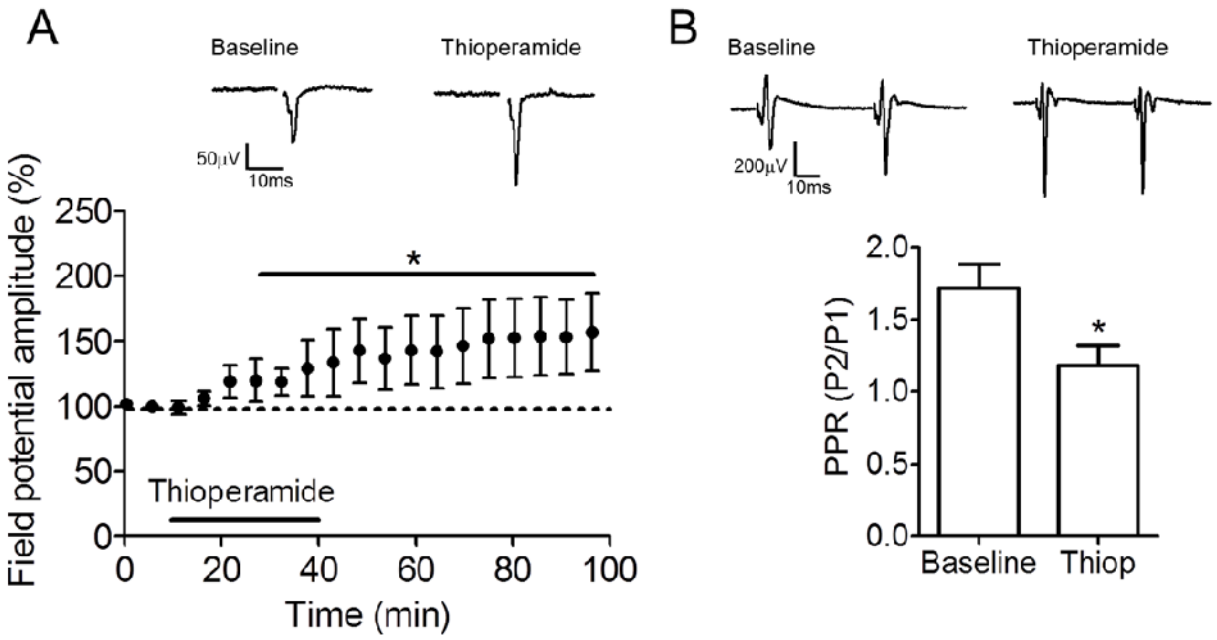

Figure 7. Effect of the H3R inverse agonist thioperamide on excitatory cortico-striatal synaptic transmission. A) Long-lasting enhancement of synaptic transmission and B) decrease in paired-pulse facilitation ratio induced by thioperamide. Excitatory field potentials (fEPSP) were evoked by either single (A) or paired (B) stimuli of cortico-striatal afferents. As shown in A, thioperamide (100nM, 30min) induced a slow-onset increase in fEPSP amplitude which continued up to 20min after washout. On the graph, data are means ± SEM (n = 3-5 slices obtained from different animals) of fEPSP amplitudes normalized to their respective baseline activity. In B, pooled paired-pulse facilitation ratio measured 5 min before and 20 min after thioperamide washout are shown. Paired-pulse facilitation was obtained by delivering two stimuli with a 50ms interval. Paired-pulse facilitation ratio was further calculated by dividing the second peak amplitude (P2) by the first one (P1). On the graph, data are expressed as averages of paired-pulse ratios (P2/P1) ± SEM obtained from 5 individual experiments where each determination is the mean of 8 consecutive fEPSP. The decrease of the paired-pulse ratio suggests that presynaptic H_3R alter the probability of neurotransmitter release. Representative electrophysiological traces are shown above each graph. They were extracted during baseline activity and 20min after thioperamide washout when signals reached a stable amplitude. In both A and B changes were statistically significant (* $p<0.05$ versus controls, repeated measures ANOVA).

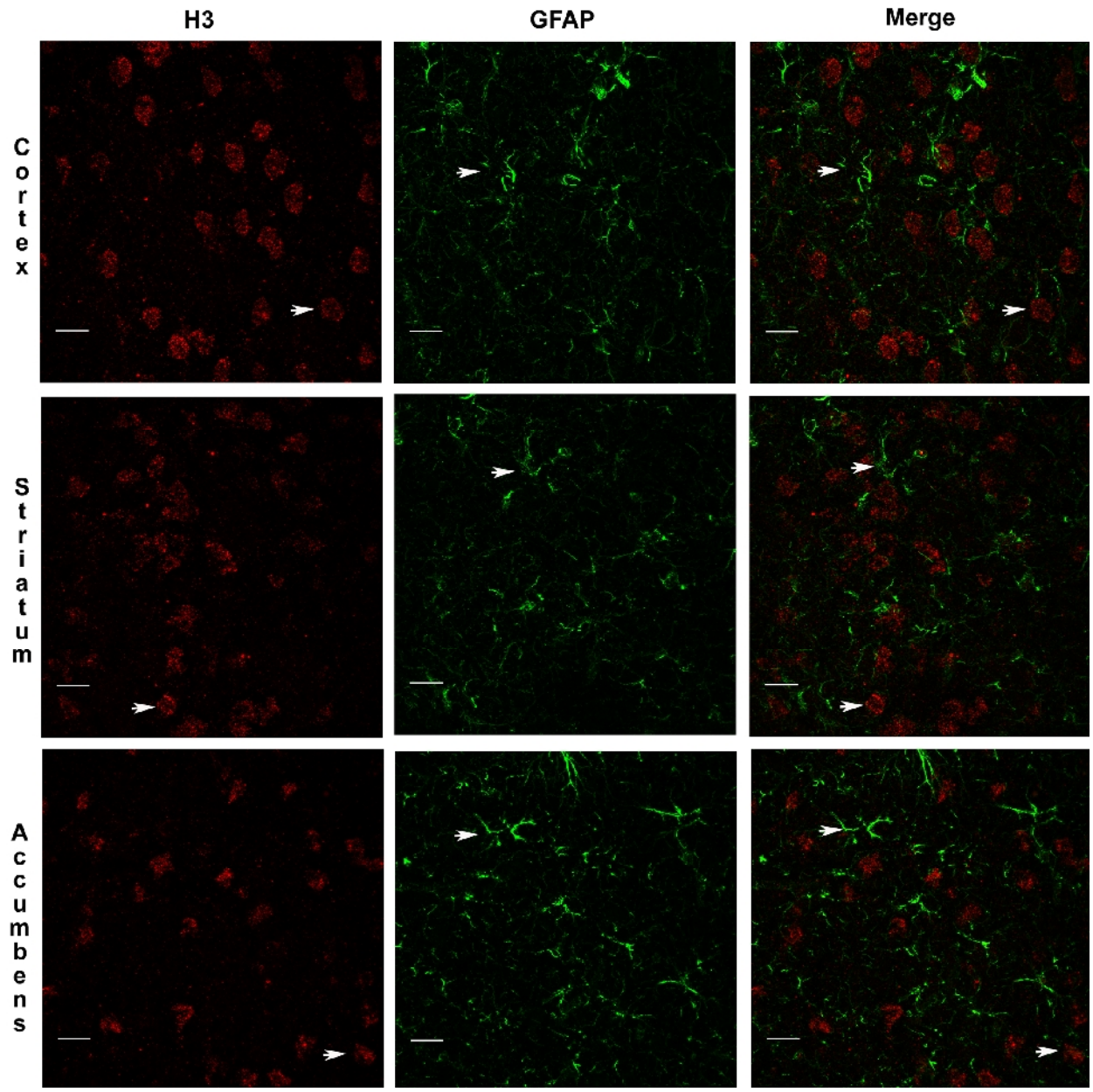

Figure 8. Absence of H_3R protein expression in astrocytes (GFAP-immunoreactive cells) in the rat forebrain. GFAP-positive astrocytes surround H_3R immunolabelled neurons in the medial prefrontal cortex, striatum and nucleus accumbens. Overlap values obtained were always lower than 0.5, the preestablished threshold to detect colocalization. Images are representative of three brain sections obtained from different animals. H_3R protein is detected as red fluorescence obtained with the Alpha Diagnostic rabbit anti-H_3R antibody followed by an anti-rabbit-peroxidase and the TSA-Cy3 system. GFAP protein is detected as green fluorescence obtained with the mouse anti-GFAP antibody developed with the goat anti-mouse-Alexa488 antibody. White arrows show immunostained cells for only one of the antigens. Scale bar 20µm.

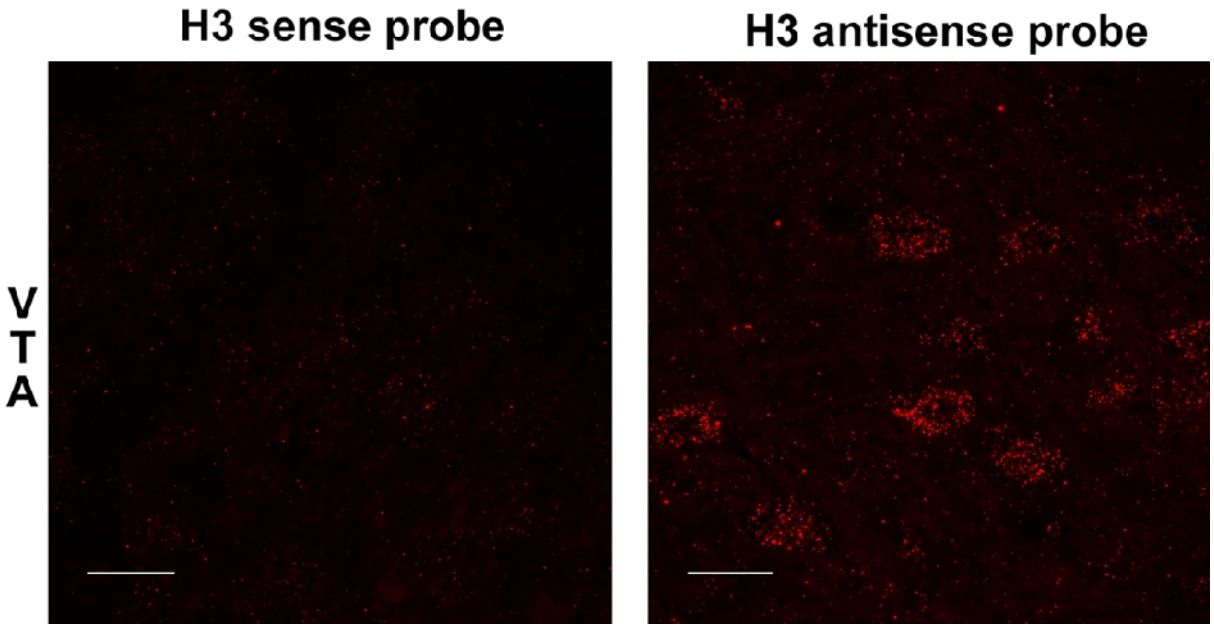

Figure S1. Comparison between sense and antisense H_3R cRNA probes. A faint signal due to low non-specific binding of the sense H_3R cRNA probe can be found in the VTA, but it is almost undetectable when compared with the specific signal. Scale bar 35µm.

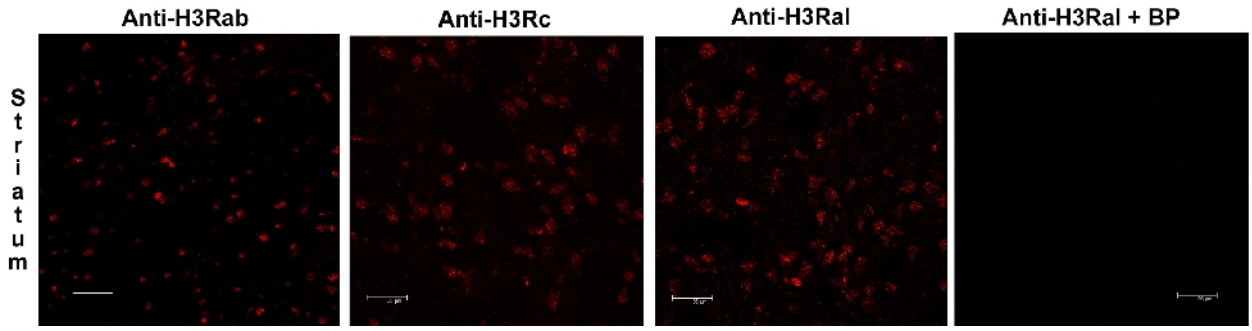

Figure S2. Comparison among diverse H_3R commercial antibodies. Similar H_3R immunostaining pattern was obtained by using three different commercial antibodies. Alpha Diagnostic anti-H3R (anti-H3Ral) signal was completely abolished by preincubation with its blocking peptide. See Table 1 for antibody details. Scale bar 35µm.